

SRG-Net: Unsupervised Segmentation for Terracotta Warrior Point Cloud with 3D Pointwise CNN methods

Yao Hu^a, Guohua Geng^a, Kang Li^{a,*}, Wei Zhou^{a,*}, Xingxing Hao^a, Xin Cao^a

^a*School of Information Science and Technology, Northwest University, Xi'an 710127, Shaanxi, China*

Abstract

At present, the repairing works of terracotta warriors in Emperor Qinshihuang's Mausoleum Site Museum are mainly done by handwork. However, with the increasing amount of unearthed pieces of terracotta warriors, the restoration efficiency of archaeologists is greatly reduced. We hope to segment the 3D point cloud data of the terracotta warriors automatically, and store the fragment data in the database to assist the archaeologists to match the actual fragments with the fragments in the database, thus could result in the higher repairing efficiency of terracotta warriors for archaeologists. Besides, previous neural network researches in 3D are mainly about supervised classification, clustering, unsupervised representation and reconstruction. There are few researches focusing on unsupervised point cloud part segmentation. To address these problems, we present a seed-region-growing CNN(SRG-Net) for unsupervised part segmentation with 3D point clouds of terracotta warriors. Firstly, we propose our customized seed region growing algorithm to coarsely segment the point cloud. Then we present our supervised segmentation and unsupervised reconstruction networks to better understand the characteristics of 3D point clouds. Finally, we combine the SRG algorithm with our improved CNN using a refinement method called SRG-Net to conduct the segmentation tasks on the terracotta warriors. Our proposed SRG-Net are evaluated on the terracotta warriors data and the benchmark dataset of ShapeNet with measuring mean intersection over union(mIoU) and latency. The experimental results show that our SRG-Net outperforms the state-of-the-art methods. Our code is available at <https://github.com/hyoau/SRG-Net>.

Keywords: Point Cloud, Unsupervised Segmentation, Terracotta Warrior, CNN, Seed Region Growing

1. Introduction

Nowadays, the repairing works of terracotta warriors are mainly accomplished by the handwork of archaeologists at the Emperor Qinshihuang's Mausoleum Site Museum. However, with more and more fragments of terracotta warriors unearthed from the archaeological site, the restoration efficiency of terracotta warriors is extremely low. Moreover, the lack of archaeological technicians to repair the terracotta warriors has exacerbated this situation. As a result, there are large amounts of fragments excavated from the archaeological site remaining to be repaired. Fortunately, with the development of 3D sensors (Apple Li-DAR, Kinect and RealSense) and the improvement of hardware (GPU and CPU) performance, it is possible to digitize the terracotta warriors. We can segment the 3D object of the terracotta warriors

*Corresponding author

Email addresses: huyao@stumail.nwu.edu.cn (Yao Hu), gengguohua@nwu.edu.cn (Guohua Geng), likang@nwu.edu.cn (Kang Li), mczhouwei12@gmail.com (Wei Zhou), ystar1991@126.com (Xingxing Hao), xin_cao@163.com (Xin Cao)

and store the fragments in the database of the museum. The researchers in the museum can match fragments excavated from the excavation site with the pre-segmented fragments in the database to restore the terracotta warriors. In order to improve the efficiency of the repairing work, we propose an unsupervised 3D point cloud segmentation method for the terracotta warrior data. With the segmentation method proposed in this paper, the complete terracotta warriors can be segmented into the fragments corresponding to various parts automatically, e.g. head, hand and foot, etc. Compared with the traditional manual method, the method proposed in this paper can greatly improve the efficiency and accuracy of the repair process.

3D data can usually be expressed in different formats, such as point clouds, meshes, volumetrics and multi-view images. Regarding which data format is used to process the model, we compare the commonly used data formats. For the mesh, it is irregular and time-consuming, which will cause high space and time complexity. Therefore, mesh is not a good way to learn the features. As for multi-view images, one image can only show the feature of one surface, but not the overall structure of an object. Recently, there have been many researches focusing on how to voxelize the point clouds to make them evenly distributed in regular 3D space, and then implement 3D-CNN on them. However, voxelization owns the high space and time complexity, and there may be quantization errors in the process of voxelization, which would result in low accuracy. Compared with other data formats, point cloud is a data structure suitable for 3D scene calculation of terracotta warriors. We choose to segment the terracotta warriors in the form of point clouds (see samples in Figure 1).



Figure 1: Simplified Terracotta Warrior Point Clouds

Our terracotta warriors are represented with $\{x_n \in R^p\}_{n=1}^N$, where R^p is the feature space, x_n means the features of one point, such as x, y, z, N_x, N_y, N_z (xyz coordinates and normal value), N means the number of points in one terracotta warrior 3D object. Our goal is to design a function $f : R^p \rightarrow L$, where L means the segmentation mapping labels. $\{c_n \in L\}_{n=1}^N$, where c_n is each point's label after the segmentation. In our problem, $\{c_n\}$ is fixed while the mapping function f and $\{x_n\}$ are trainable, so this problem can also be regarded as a supervised problem. To solve the unsupervised segmentation problem, we can split the problem into two sub-problems. Firstly, we need to design

an algorithm to make prediction of optimal L . Secondly, we need to design a network to better learn the labels $\{c_n\}$ and make the most of the terracotta warrior point cloud features. To get the optimal cluster labels $\{c_n\}$, we think that a good point cloud segmentation acts like what a human does. Similar to image segmentation [1], when a person is asked to segment a point cloud, he is most likely to cluster the points according to the similar features or semantic meaning of different parts. In 2D images, spatially continuous pixels tend to have similar colors or texture. While in 3D point cloud, grouping spatially continuous points that have similar normal value or colors are reasonable to be given the same label in 3D point cloud segmentation. Besides, the euclidean distance between the points will not be very long. In conclusion, we design two criteria to predict the $\{c_n\}$:

1. Points with similar features are desired to be given the same label.
2. The euclidean distance between spatially continuous points should not be quite long.

We design a SRG algorithm to learn the normal feature of point clouds as much as possible. The experiment [2] shows that the encode-decoder structure of FoldingNet[3] does help neural network learn from point cloud. And DG-CNN is good at learning local features. So we combine **FoldingNet** [3] and **DG-CNN** [4] to better learn the part feature of terracotta warriors. In Section3, we describe the details of the process of assigning labels $\{c_n\}$. Section4 will show that our method achieve better methods compared with other methods. Compared with existing methods, the key contribution of our work can be summarized as follows:

- We design a novel SRG algorithm for point cloud segmentation to make the most of point cloud xyz coordinates by estimating normal feature.
- We design our CNN by combining DG-CNN and FoldingNet to better learn the local and global features of 3D point clouds.
- We combine the SRG algorithm and CNN neural network with our refinement method and achieve state-of-the-art segmentation results.
- Our end-to-end model not only can be used in terracotta warrior point clouds, but also can obtain quite good results on other point clouds and we evaluate our SRG-Net on ShapeNet dataset.

2. Related Work

Segmentation is common both in 2D images and 3D point clouds. In 2D image, segmentation accomplish a task that assigns labels to all the pixels in one image to cluster the pixels with feature. Similarly, point cloud segmentation is a process assigning labels to all the points in point cloud. The expected result is the points with similar feature are assigned with the same label.

In terms of image segmentation, k-means is a classical segmentation method in both 2D and 3D, which leads to partition n observations into k clusters with the nearest mean. This method is quite popular in data mining. Graph-based method is another popular method like Prim and Kruskal [5] which implements simple greedy decisions in

segmentation. The above methods focus on global features instead of the local differentiate features, so when it comes to the complex context, usually they cannot get promising results. Among unsupervised deep learning methods, there are many methods learning feature using the generative methods, such as [6, 7, 8]. They follow the model of neuroscience, where each neuron represents specific semantic meaning. Meanwhile, CNN is widely used in image unsupervised segmentation. For example, in [1], Kanezaki combines the superpixel [9] method and CNN, and employs superpixel for back propagation to tune the unsupervised segmentation results. Besides, [10] uses a spatial continuity loss as an alternative to settle the limitation of the former work [9], whose method is also quite useful in 3D point cloud feature learning.

In the field of 3D point cloud segmentation, the state-of-the-art methods for 2D images is not quite suitable for being directly used on point cloud because 3D point cloud segmentation requires the understanding both the global feature and geometric details of each point. 3D point cloud segmentation methods can be classified into three types: semantic segmentation, instance segmentation and object segmentation. Semantic segmentation focuses on scene level segmentation, instance segmentation lay particular emphasis on object level segmentation, and object segmentation is centered on part level segmentation.

As to semantic segmentation, semantic segmentation aims at separating a point cloud into several parts with the semantic meaning of each point. There are four main paradigms in semantic segmentation including projection-based methods, discretization-based methods, point-based methods and hybrid methods. Projection-based methods always project a 3D point cloud to 2D images, such as multi-view [11, 12], spherical [13, 14]. Discretization-based method usually project a point cloud into a discrete representation, such as volumetric [15] and sparse permutohedral lattices [16, 17]. Instead of learning a single feature on 3D scans, several methods try to learn different features from 3D scans, such as [16, 18, 17].

Point-based network can directly learn features on a point cloud and separate it into several parts. Point clouds are irregular, unordered and unstructured. PointNet [19] can directly learn features from point cloud and retain the point cloud permutation invariance with a symmetric function like maximum function and sum function. PointNet can learn point wise feature with the combination of several MLP layers and a max-pooling layer. PointNet is a pioneer that directly learn on point cloud. A series of point-based network has been proposed based on PointNet. However, PointNet can only learn features on each point instead on the local structure. So PointNet++ is presented to get local structure from neighborhood with a hierarchy network [20]. PointSIFT [21] is proposed to encode orientation and reach scale awareness. Instead of using K-means to cluster and KNN to generate neighborhoods like the grouping method PointNet++, PointWeb [22] is proposed to get the relations between all the points constructed in a local fully-connected web. As to convolution based method. RS-CNN takes a local point cloud subset as its input and maps the low-level relation to high level relation as the convolution to better learn the feature. PointConv [23] uses the existing algorithm, using a Monte Carlo estimation to define the convolution. PointCNN [24] uses $\chi - conv$ transformation to convert point cloud into a latent and cananical order. As to point convolution methods, Parametric Continuous Convolutional Neural Network(PCCN) [25] is proposed based on a parametric continuous convolution layers, whose kernel function is parameterized by MLPs and spans the continuous vector space. As to Graph based method, compared

with other methods, graph-based methods can better learn the features like shapes and geometric structures in point clouds. Graph Attention Convolution(GAC) [26] can learn several relevant features from local neighborhoods by dynamically assigning attention weights to points in different neighborhoods and feature channels. Dynamic Graph CNN(DG-CNN) [4] constructs several dynamic graphs in neighborhood, and concatenate the local and global features to extract better features and update each graph after each layer of the network dynamically. FoldingNet adopts the auto-encoder structure to encode the point cloud $N \times 3$ to 1×512 and decode it to $M \times 3$ with the aid of chamfer loss to construct the auto-encoder network.

In terms of part segmentation, compared with semantic and instance segmentation, part segmentation is more difficult because there are large geometric differences between the points with the same labels and the number of parts with the same semantic meanings may differ. Z. Wang et al. [27] propose VoxSegNet to achieve promising part segmentation results on 3D voxelized data, which proposes a Spatial Dense Extraction(SDE) module to extract multi-scale features from volumetric data. Synchronized Spectral CNN (SyncSpecCNN) [28] is proposed to achieve fine-grained part segmentation on irregularity and non-isomorphic shape graphs with convolution. [29] is proposed to segment unorganized noisy point clouds automatically by extracting clusters of points on the Gaussian sphere. [30] uses three shape indexes: the smoothness indicator, shape index and flatness index, which is based on a fuzzy parameterization. [31] present a segmentation method for conventional engineering objects based on local estimates of various geometric features. Branched AutoEncoder network (BAE-NET) [32] is proposed to perform unsupervised and weakly supervised 3D shape co-segmentation. Each branch of the network can learn features from a specific part shape for a specific part shape with representation, based on the auto-encoder structure.

3. Proposed Method

In this paper, our input data for terracotta warrior is the form of 3D point clouds (see also samples in Figure 1). A point cloud is represented as a set of 3D points $\{P_i | i = 1, 2, 3, \dots, n\}$, where each point is a vector R^n containing coordinates x, y, z and other features like normal, color. Our method contains three steps:

1. We estimate normal value with the xyz coordinates.
2. We use our seed region growing method to pre-segment the point cloud.
3. We use our pointwise CNN called SRG-Net self-trained to segment the point cloud with the refinement of pre-segmentation results.

Given a point cloud only with 3D coordinates, there are several effective normal estimation methods like [33] [34] [35]. In our method, we follow the simplest method in [36] because of its low average-case complexity and quite good accuracy. We propose an unsupervised segmentation method for the terracotta warrior point cloud by combining our seed-region-growing clustering method with our 3D pointwise CNN called SRG-Net. This method contains two phases, SRG segmentation and CNN deep learning. The problem we want to solve can be described as follows. First, SRG algorithm is implemented on the point cloud to do pre-segmentation. Then we use SRG-Net to self-train for unsupervised with pre-segmentation labels of SRG.

3.1. Seed Region Growing

Unlike 2D images, not all point cloud data has features such as color and normal. For example, our terracotta warriors 3D object do not have any color feature. However, normal vectors can be calculated and predicted by point coordinates. It is worth noting that there are many similarities and differences between color in 2D and normal features in 3D. For color feature in 2D image, if the pixels are semantically related, the color of the pixel in the neighborhood generally do not change. For 3D point cloud normal features, compared with the color features in 2D images, the normal values of points in the neighborhood of the point cloud often differs. In terms of similarities, even though each point of point cloud neighborhood has different normal values, they usually do not change much unless they are not semantically continuous. We design a seed-region-growing method to pre-segment the point cloud based on the above characteristics of the normal feature of point cloud.

Algorithm 1: SRG unsupervised segmentation

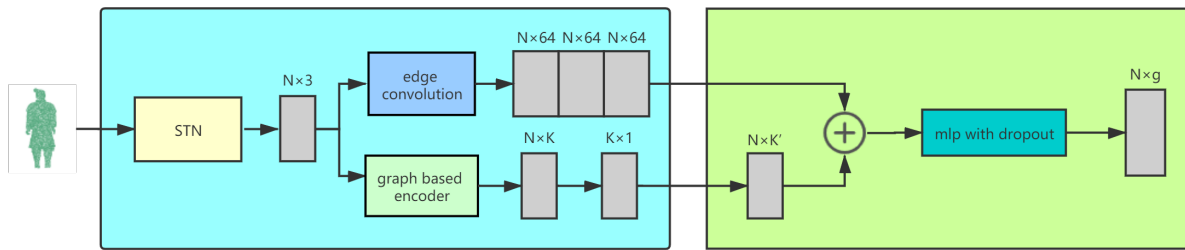
```

Input:  $P = \{p_n \in R^3\}$  // x, y, z coordinates
          $N = \{n_n \in R^3\}$  // normal value
          $E = \{e_n \in R^n\}$  // euclidean distance
          $\Omega(\cdot)$  // nearest neighbour function
Output:  $L = \{l_n \in R^1\}$  // segmentation label of each point
Initialize:  $S := \emptyset$  // set seed list to empty
          $A := \text{rand}\{1, 2 \dots |P|\}$  // select random point to available point list as seed
for  $t = 1$  to  $T$  do
    while  $A \neq \emptyset$  do
         $a \leftarrow \text{first item in } A$ 
         $\text{neighbours} \leftarrow \Omega(a)$  for  $\text{neighbours} \neq \emptyset$  do
             $\text{neighbour} \leftarrow \text{rand}(\text{neighbours})$ 
            if  $E(a, \text{neighbour}) \leq e_{th} \wedge N(a, \text{neighbour}) \leq n_{th} \wedge \text{neighbour} \notin S$  then
                 $\text{append neighbour to } S$   $\text{remove neighbour from neighbours}$ 
            else
                 $\text{remove neighbour from neighbours}$ 
         $\text{add } a$  to  $S$ 

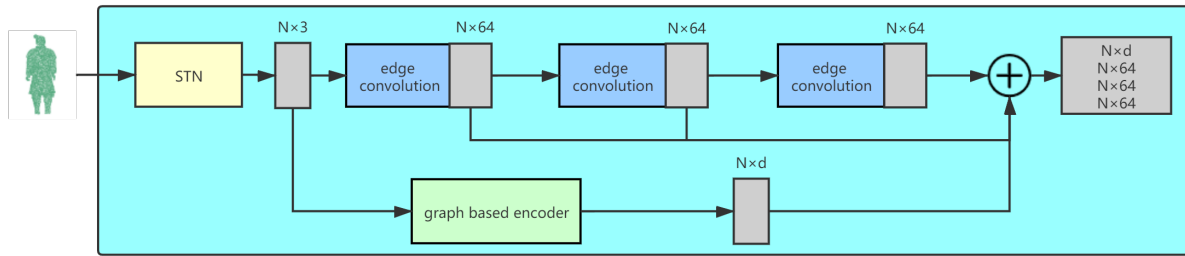
```

First, we implement KNN to the point cloud to the point cloud to get the nearest neighbors of each point. Then we pick up a random point as the start seed and add to the available points to start the algorithm. Then we choose the first seed from the available list to judge the points in its neighborhood. If the normal value and euclidean distance are within the threshold we set, then it can be judged that the two points are semantically continuous and we can group two points into one cluster. An outline about the SRG-clustering is given in **Algorithm 1**. The description of the algorithm is as follows:

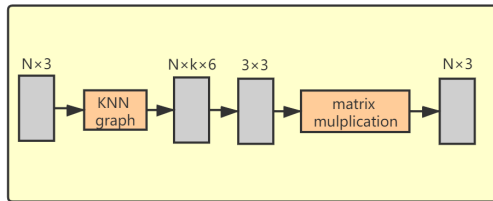
1. Input:
 - (a) xyz coordinates of each point $p_n \in R^3$



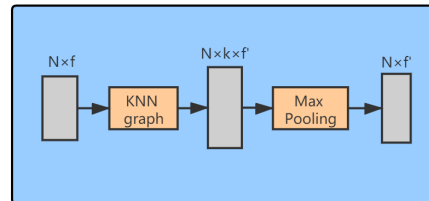
(a) Network Structure



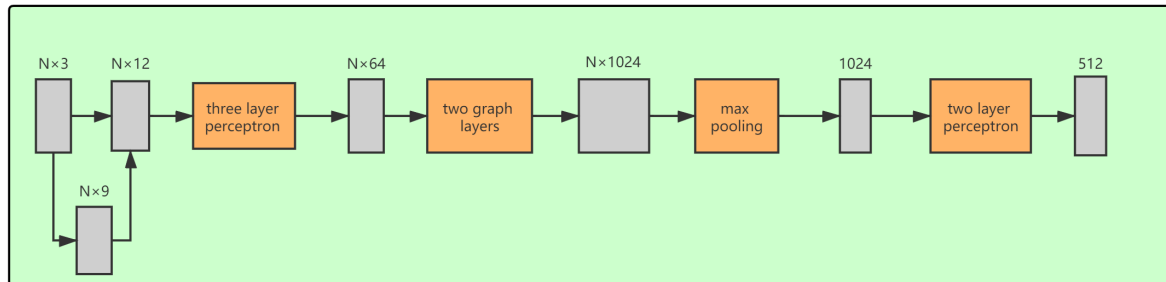
(b) Encoder



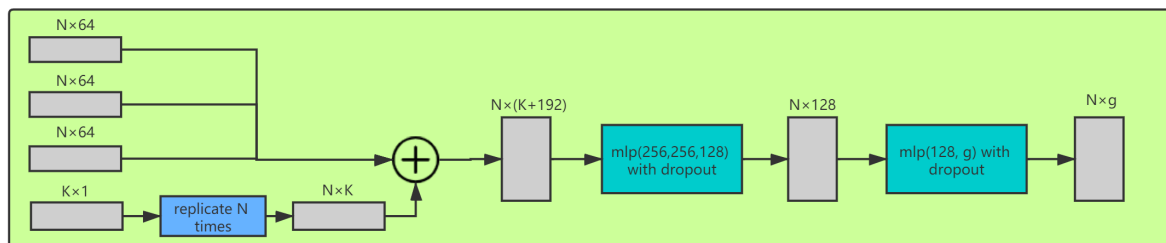
(c) STN



(d) Edge Convolution



(e) Graph Based Encoder



(f) Segmenter

Figure 2: Network Structure

- (b) normal value of each point $n_n \in R^3$
 - (c) euclidean distance of every two points $e_n \in R^n$
 - (d) neighborhood of each point $b_n \in R^k$
2. The random chosen point is added to the set A , we can call it seed a .
 3. For other points which are not transformed to seeds in A :
 - (a) Each of point in seed’s neighbor N_a , check the normal distance and euclidean distance between the point in N_a and the seed a .
 - (b) We set the normal distance and the euclidean distance threshold. If both of the two value is less than the two threshold, we can add it to A .
 - (c) The current seed is added to checked list S .

3.2. SRG-Net

We propose our SRG-Net, which is inspired by dynamic graph in DG-CNN and auto-encoder in FoldingNet. Unlike classical graph CNN, our graph is dynamic and updated in each layer of the network. Compared with the methods that purely focus on the relation-ship between points, we also propose an encoder structure to better express the features of the entire point cloud, aiming at better learn the structure of the point cloud and optimize the pre-segmentation results of SRG. Our network structure can be shown in Figure2, which consists of two sub-network, the first part is encoder that generate features from dynamic graph and the whole point cloud while the second is the segmentation network.

We denote the point cloud as S . We use lower-case letters to represent vectors, such as x , and use upper-case letter to represent matrix, such as A . We call a matrix m-by-n or $m \times n$ if it has m rows and n columns. In addition, the terracotta warrior point cloud data is N points with 6 features x, y, z, N_x, N_y, N_z (xyz coordinates and normal value), denoted as $X = \{x_1, x_2, x_3, \dots, x_n\} \subseteq R^6$.

3.2.1. Encoder Architecture

The SRG-Net encoder follows a similar design of [3], the structure of SRG-Net is shown Figure 2. Compared with [3], our encoder concatenate several multi-layer perceptrons(MLP) and several dynamic graph-based max-pooling layers. The dynamic graphs are constructed by applying KNN on point clouds.

First, for the entire point cloud. We compute a spatial transformer network and get a transformer matrix of 3-by-3 to maintain invariance under transformations. Then for the transformed point cloud, we compute three dynamic graphs and get graph features respectively. In graph feature extracting process, we adopt the Edge Convolution in [7] to compute the graph feature of each layer, which uses an asymmetric edge function in Eq. (1):

$$f_{ij} = h(x_i, x_i - x_j) \quad (1)$$

where it combines the coordinates of neighborhood center x_i with the subtraction of neighborhood point and the center point coordinates $x_i - x_j$ to get local and global information of neighborhood. Then we define our operation in Eq. (2):

$$g_{ij} = \Theta(\mu \cdot (x_i - x_j) + \omega \cdot x_i) \quad (2)$$

where μ and ω are parameters and Θ is a ReLU function. Eq. (2) is implemented as a shared MLP with Leaky ReLU. Then we define our max-pooling operation in Eq. (3):

$$x_i = \max_{j \in N(i)} g_{ij} \quad (3)$$

where $N(i)$ means neighborhood of point i .

Bottleneck is computed by graph feature extraction layer, whose structure is show in Figure2. First, we compute covariance 3×3 matrix for every point and vectorize it to 1×9 . Then the $n \times 3$ matrix of point coordinates is concatenated with the $n \times 9$ covariance matrix into a $n \times 12$ matrix and enter the matrix into a 3-layer perceptron. Then we feed the output of the perceptron to two subsequent graph layers. In each layer, max-pooling is added to the neighbor of each node. At last, we apply a 3-layer perceptron to the former output and get the final output. The whole process of the graph feature extraction layer is summarized in Eq. (4):

$$Y = I_{max}(X)K \quad (4)$$

In Eq. (4), X is the input matrix to the graph layer and K is a feature mapping matrix. $I_{max}(X)$ can be represented in Eq. 5:

$$(I_{max}(X))_{ij} = \Theta(\max_{k \in N(i)} x_{kj}) \quad (5)$$

where Θ is a ReLU function and $N(i)$ is the neighborhood of point i . The max-pooling operation in Eq. (5) can get local feature based on the graph structure. So the graph feature extraction layer can not only get local neighborhood features, but also global features.

3.2.2. Segmenter Architecture

Segmenter gets dynamic graph features and bottleneck as input and assign labels to each point to segment the whole point cloud. The structure of segmenter is shown in Figure 2. First, bottleneck is replicated N times in Eq. (6):

$$B' = \underbrace{B \cup B \cup \dots \cup B}_N \quad (6)$$

where N is the number of points in point cloud and B is the bottleneck. The output of replication is concatenated with dynamic features in Eq. (7):

$$C = B' \cup D_1 \cup D_2 \cup D_3 \quad (7)$$

where D_1, D_2, D_3 represent dynamic graph features. At last, we feed the output of concatenation to a multi-layer-perceptron to segment the point cloud in Eq. (8).

$$D = \Theta(\Psi \cdot C + \Omega) \quad (8)$$

where Ψ and Ω represent parameters in linear function, and Θ represents a ReLU function.

3.3. Refinement

Instead of working on the SRG pre-segmentation results straightly, point refinement like [37] is implemented in our SRG-Net method. There is no need to set cluster number very big in SRG, because DG-CNN and FoldingNet have the ability of learning the local and global features and refinement can achieve quite better results compared with straight learning in Figure 1.

4. Experiments

We train our data on our terracotta warrior dataset and ShapeNet v2 dataset. The pipeline is implemented by using PyTorch and Python3.7. All the result is based on experiment under GeForce RTX 2080 Ti and Intel(R) Core(TM) i9-9900K CPU @ 3.60GHz. We also evaluate our pipeline on the above datasets. The performance is evaluated by mean intersection-over-union(mIoU).

In our work, the 3D models of terracotta warriors are obtained by Artec Eva [38]. We got 500 intact terracotta warriors 3D models. Each model consists of about 2 million points, verture color, verture normal, face color, wedge coordinates and texture images. We convert the 3D obj files to point clouds with x, y, z and estimate normal value N_x, N_y, N_z to aid to our segmentation work. We also down sample our point clouds to 10,000 points to limit the memory under 11GB. In order to evaluate our method, we also split the models into three parts, 80% models for training, 20% for testing. Some of our simplified 3D models are shown in Figure 1. In order to further evaluate our method, we also test our data on ShapeNet [39].

4.1. Experiments on Terracotta Warrior

In our experiments on terracotta warrior. We got 500 intact terracotta warriors 3D models. Each model consists of about 2 million points, verture color, verture normal, face color, wedge coordinates and texture images. Firstly, We convert the 3D obj files to point clouds with x, y, z and estimate normal value N_x, N_y, N_z . Secondly, We down sample our point clouds to 10,000 points. Thirdly, we implement our SRG-Net to our terracotta warrior dataset. We set number of iterations as 2000 to achieve a balance between time-consuming and accuracy. The segmentation results of different iterations in one terracotta warrior model is shown in Figure 3.

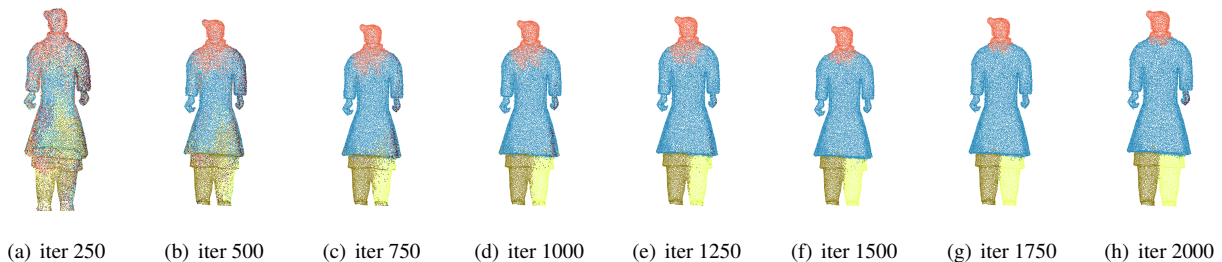


Figure 3: Results of Different Iterations in SRG-Net











































Method	005413	005420	005422	005423	005427	005455
SRG-Net						
SRG-DGCNN						
Kmeans-DGCNN						
SRG-Pointnet2						
Kmeans-Pointnet2						
SRG-Pointnet						
Kmeans-Pointnet						

Table 1: Results of Different Methods

Method	mIoU	Latency
SRG-Net	0.8263	32.11
SRG-DGCNN	0.7832	37.26
Kmeans-DGCNN	0.7064	36.30
SRG-Pointnet2	0.7055	24.10
Kmeans-Pointnet2	0.5233	25.38
SRG-Pointnet	0.7603	13.35
Kmeans-Pointnet	0.5394	13.47

Table 2: Comparison of Different Methods

4.2. Comparison of Different Methods

In this section, we compare our SRG-Net with the state-of-the-art methods sharing the similar structure of our SRG-Net. we compare our SRG-Net with the state-of-the-art methods. We choose K-means as a comparison with our seed region growing method and DG-CNN, PointNet++, PointNet as the comparison with our convolution neural network. So we compare our SRG-Net with SRG-DGCNN, SRG-PointNet++, SRG-PointNet, K-means-DGCNN, K-means-PointNet++, K-means-PointNet.

The comparison experiments are implemented on our terracotta warriors datasets. We trained these methods on 400 terracotta warriors 3D point cloud, and we test the trained model on the other 120 point clouds. According to the suggestions of experts in the school of archaeology, it is reasonable to split the intact terracotta warriors into five to seven parts. So we split the point cloud into six pieces both in SRG, K-Means. We also set segmentation number $S = 6$ and number of iterations $T = 2000$ in CNN methods(PointNet, PointNet2, DG-CNN, DGCNN-refine) for each point cloud. The results of different iterations in SRG-Net are show in Figure 3. Comparison of different methods are shown as in Table 2. The results of different methods can be shown in Table. 1.

4.3. Experiments on ShapeNet

In this section we perform experiments on ShapeNet to evaluate robustness of our SRG-Net method. The dataset contains 16,881 object from 16 categories. We set number of part according to different categories separately. Some of the unsupervised segmentation results are shown in Figure 4. As Figure 4 shows SRG-Net can segment well-structured objects such as knife, motorbike, etc. But when faced with objects that are not very well-structured such as mug, the segmentation results are not very good. We will conduct research on the robustness of SRG-Net in the future work.

5. Conclusion

In this paper, we provide an end-to-end model called SRG-Net on unsupervised segmentation for terracotta warrior point cloud, which assist the archaeologists to speed up the repairing process of terracotta warriors. Firstly, we design a novel seed region growing methods to pre-segment the point clouds by making full use of the point cloud coordinates



Figure 4: SRG-Net Segmentation Results of ShapeNet

and normal information of the 3D terracotta warriors point clouds. Based on this pre-segmentation process, we proposed a CNN which is inspired by dynamic graph in DG-CNN and auto-encoder in FoldingNet to better learn the local and global characteristics of 3D point clouds. And then we presented a refinement method, and embed it after the above two processes. Finally, we evaluate our method on the terracotta warriors data, and we outperform the state-of-the-art methods with better segmentation results and higher efficiency. Besides, we also conduct experiments on the ShapeNet dataset, which demonstrates our method is also useful in human body and normal object part segmentation.

Our work still has some limitations. Since the number of points from the hand of terracotta is quite small, it is difficult for our SRG-Net to learn the characteristics of hands. We will try to work on this problem in the future. We hope our work can be a useful tool for the research of terracotta warrior in archaeology and for other researchers' point cloud work.

6. Acknowledgments

This work is equally and mainly supported by the National Key Research and Development Program of China (No. 2019YFC1521102) and the Key Research and Development Program of Shaanxi Province (No. 2020KW-068). Besides, this work is also partly supported by the Key Research and Development Program of Shaanxi Province (No. 2019GY-215), the Major research and development project of Qinghai(No. 2020-SF-143), the National Natural Science Foundation of China under Grant (No.61701403) and the Young Talent Support Program of the Shaanxi Association for Science and Technology under Grant (No.20190107).

References

- [1] A. Kanezaki, Unsupervised image segmentation by backpropagation, in: 2018 IEEE international conference on acoustics, speech and signal processing (ICASSP), IEEE, 2018, pp. 1543–1547.
- [2] A. Tao, Unsupervised point cloud reconstruction for classic feature learning, <https://github.com/AnTao97/UnsupervisedPointCloudReconstruction>.
- [3] Y. Yang, C. Feng, Y. Shen, D. Tian, Foldingnet: Point cloud auto-encoder via deep grid deformation, in: Proceedings of the IEEE Conference on Computer Vision and Pattern Recognition, 2018, pp. 206–215.
- [4] Y. Wang, Y. Sun, Z. Liu, S. E. Sarma, M. M. Bronstein, J. M. Solomon, Dynamic graph cnn for learning on point clouds, *Acm Transactions On Graphics (tog)* 38 (5) (2019) 1–12.
- [5] J. B. Kruskal, On the shortest spanning subtree of a graph and the traveling salesman problem, *Proceedings of the American Mathematical society* 7 (1) (1956) 48–50.
- [6] H. Lee, P. Pham, Y. Largman, A. Ng, Unsupervised feature learning for audio classification using convolutional deep belief networks, *Advances in neural information processing systems* 22 (2009) 1096–1104.

- [7] Q. V. Le, Building high-level features using large scale unsupervised learning, in: 2013 IEEE international conference on acoustics, speech and signal processing, IEEE, 2013, pp. 8595–8598.
- [8] H. Lee, R. Grosse, R. Ranganath, A. Y. Ng, Convolutional deep belief networks for scalable unsupervised learning of hierarchical representations, in: Proceedings of the 26th annual international conference on machine learning, 2009, pp. 609–616.
- [9] R. Achanta, A. Shaji, K. Smith, A. Lucchi, P. Fua, S. Süsstrunk, Slic superpixels compared to state-of-the-art superpixel methods, IEEE transactions on pattern analysis and machine intelligence 34 (11) (2012) 2274–2282.
- [10] W. Kim, A. Kanezaki, M. Tanaka, Unsupervised learning of image segmentation based on differentiable feature clustering, IEEE Transactions on Image Processing 29 (2020) 8055–8068.
- [11] F. J. Lawin, M. Danelljan, P. Tosteberg, G. Bhat, F. S. Khan, M. Felsberg, Deep projective 3d semantic segmentation, in: International Conference on Computer Analysis of Images and Patterns, Springer, 2017, pp. 95–107.
- [12] A. Boulch, B. Le Saux, N. Audebert, Unstructured point cloud semantic labeling using deep segmentation networks., 3DOR 2 (2017) 7.
- [13] B. Wu, A. Wan, X. Yue, K. Keutzer, Squeezeseg: Convolutional neural nets with recurrent crf for real-time road-object segmentation from 3d lidar point cloud, in: 2018 IEEE International Conference on Robotics and Automation (ICRA), IEEE, 2018, pp. 1887–1893.
- [14] A. Milioto, I. Vizzo, J. Behley, C. Stachniss, Rangenet++: Fast and accurate lidar semantic segmentation, in: 2019 IEEE/RSJ International Conference on Intelligent Robots and Systems (IROS), IEEE, 2019, pp. 4213–4220.
- [15] B. Graham, M. Engelcke, L. Van Der Maaten, 3d semantic segmentation with submanifold sparse convolutional networks, in: Proceedings of the IEEE conference on computer vision and pattern recognition, 2018, pp. 9224–9232.
- [16] A. Dai, M. Nießner, 3dmv: Joint 3d-multi-view prediction for 3d semantic scene segmentation, in: Proceedings of the European Conference on Computer Vision (ECCV), 2018, pp. 452–468.
- [17] M. Jaritz, J. Gu, H. Su, Multi-view pointnet for 3d scene understanding, in: Proceedings of the IEEE International Conference on Computer Vision Workshops, 2019, pp. 0–0.
- [18] S. Wang, S. Suo, W.-C. Ma, A. Pokrovsky, R. Urtasun, Deep parametric continuous convolutional neural networks, in: Proceedings of the IEEE Conference on Computer Vision and Pattern Recognition, 2018, pp. 2589–2597.
- [19] C. R. Qi, H. Su, K. Mo, L. J. Guibas, Pointnet: Deep learning on point sets for 3d classification and segmentation, in: Proceedings of the IEEE conference on computer vision and pattern recognition, 2017, pp. 652–660.

- [20] C. R. Qi, L. Yi, H. Su, L. J. Guibas, Pointnet++: Deep hierarchical feature learning on point sets in a metric space, in: *Advances in neural information processing systems*, 2017, pp. 5099–5108.
- [21] M. Jiang, Y. Wu, T. Zhao, Z. Zhao, C. Lu, Pointsift: A sift-like network module for 3d point cloud semantic segmentation, arXiv preprint arXiv:1807.00652.
- [22] H. Zhao, L. Jiang, C.-W. Fu, J. Jia, Pointweb: Enhancing local neighborhood features for point cloud processing, in: *Proceedings of the IEEE Conference on Computer Vision and Pattern Recognition*, 2019, pp. 5565–5573.
- [23] W. Wu, Z. Qi, L. Fuxin, Pointconv: Deep convolutional networks on 3d point clouds, in: *Proceedings of the IEEE Conference on Computer Vision and Pattern Recognition*, 2019, pp. 9621–9630.
- [24] Y. Li, R. Bu, M. Sun, W. Wu, X. Di, B. Chen, Pointcnn: Convolution on \mathcal{X} -transformed points (2018). arXiv: 1801.07791.
- [25] S. Wang, S. Suo, W.-C. Ma, A. Pokrovsky, R. Urtasun, Deep parametric continuous convolutional neural networks, in: *Proceedings of the IEEE Conference on Computer Vision and Pattern Recognition*, 2018, pp. 2589–2597.
- [26] P. Veličković, G. Cucurull, A. Casanova, A. Romero, P. Lio, Y. Bengio, Graph attention networks, arXiv preprint arXiv:1710.10903.
- [27] Z. Wang, F. Lu, Voxsegnet: Volumetric cnns for semantic part segmentation of 3d shapes, *IEEE transactions on visualization and computer graphics*.
- [28] L. Yi, H. Su, X. Guo, L. J. Guibas, Syncspecnn: Synchronized spectral cnn for 3d shape segmentation, in: *Proceedings of the IEEE Conference on Computer Vision and Pattern Recognition*, 2017, pp. 2282–2290.
- [29] Y. Liu, Y. Xiong, Automatic segmentation of unorganized noisy point clouds based on the gaussian map, *Computer-Aided Design* 40 (5) (2008) 576–594.
- [30] L. Di Angelo, P. Di Stefano, Geometric segmentation of 3d scanned surfaces, *Computer-Aided Design* 62 (2015) 44–56.
- [31] P. Benkő, T. Várady, Segmentation methods for smooth point regions of conventional engineering objects, *Computer-Aided Design* 36 (6) (2004) 511–523.
- [32] Z. Chen, K. Yin, M. Fisher, S. Chaudhuri, H. Zhang, Bae-net: Branched autoencoder for shape co-segmentation, in: *Proceedings of the IEEE International Conference on Computer Vision*, 2019, pp. 8490–8499.
- [33] D. OuYang, H.-Y. Feng, On the normal vector estimation for point cloud data from smooth surfaces, *Computer-Aided Design* 37 (10) (2005) 1071–1079.
- [34] J. Zhou, H. Huang, B. Liu, X. Liu, Normal estimation for 3d point clouds via local plane constraint and multi-scale selection, *Computer-Aided Design* 129 (2020) 102916.

- [35] Y. Wang, H.-Y. Feng, F.-É. Delorme, S. Engin, An adaptive normal estimation method for scanned point clouds with sharp features, *Computer-Aided Design* 45 (11) (2013) 1333–1348.
- [36] R. B. Rusu, S. Cousins, 3d is here: Point cloud library (pcl), in: 2011 IEEE international conference on robotics and automation, IEEE, 2011, pp. 1–4.
- [37] A. Kanezaki, Unsupervised image segmentation by backpropagation, in: 2018 IEEE international conference on acoustics, speech and signal processing (ICASSP), IEEE, 2018, pp. 1543–1547.
- [38] A. Europe, 3d object scanner artec eva — best structured-light 3d scanning device.
URL <https://www.artec3d.com/portable-3d-scanners/artec-eva>
- [39] A. X. Chang, T. Funkhouser, L. Guibas, P. Hanrahan, Q. Huang, Z. Li, S. Savarese, M. Savva, S. Song, H. Su, et al., Shapenet: An information-rich 3d model repository, *arXiv preprint arXiv:1512.03012*.